

Direct experimental evidence for the role of oxygen in the luminescent properties of GaN

M. Toth, K. Fleischer,* and M. R. Phillips†

Microstructural Analysis Unit, University of Technology, Sydney, P.O. Box 123, Broadway, NSW 2007, Australia

(Received 28 September 1998)

We present experimental evidence of electron-beam-induced diffusion of O and H in unintentionally doped *n*-type GaN grown on a sapphire substrate. Impurity diffusion was investigated using cathodoluminescence kinetics and imaging at 4 and 300 K and by wavelength dispersive x-ray analysis. The results illustrate the significance of electron-beam-induced electromigration in wide band gap semiconductors, confirm the roles of O_N^\bullet in bound exciton, donor-acceptor pair and yellow emissions and suggest the involvement of O_N^\bullet and hydrogenated gallium vacancies in the previously unexplained blue luminescence. [S0163-1829(99)09403-5]

GaN is a promising candidate for high-power, high-temperature optoelectronic devices. Device performance can, however, be limited by parasitic defect-induced emissions such as the yellow luminescence (YL) observed in autodoped GaN.¹ Unintentionally doped GaN is generally strongly *n* type primarily due to high concentrations of shallow donor Si_{Ga}^\bullet and O_N^{1-3} . YL has been attributed to a shallow donor-deep acceptor transition.⁴ First-principles total-energy calculations have shown that the most energetically favorable native deep acceptor in *n*-type GaN is the gallium vacancy (V_{Ga}'''), which has been proposed to be involved in YL.^{1,2} These calculations are consistent with positron annihilation and photoluminescence experiments that have demonstrated a correlation between V_{Ga}''' concentration and YL intensity.⁵ V_{Ga}''' can form a complex with the nearest-neighbor O_N^\bullet and a less stable complex with the second nearest-neighbor Si_{Ga}^\bullet .¹ $(V_{Ga}-O_N)''$ and $(V_{Ga}-Si_{Ga})''$ complexes have low-formation energies and are therefore expected to play significant roles in YL generation.^{1,2}

Up to four H impurities can be incorporated at a gallium vacancy.⁶ The presence of H causes the vacancy energy levels to split and shift towards the valence band until, in the limiting case of $(V_{Ga}-H_4)^\bullet$, all the levels shift into the valence band.⁶ We present experimental evidence of electron-beam-induced diffusion of O and H in autodoped (*n*-type) GaN. The results confirm the roles of O in YL, donor-acceptor pair, and bound exciton emissions and suggest the involvement of O and hydrogenated gallium vacancies in the previously unexplained blue luminescence (BL) in *n*-type GaN.

The sample used in this study was an unintentionally *n*-doped 4- μ m epilayer of wurtzite GaN grown at 1040 °C on a 25-nm GaN buffer layer by metal-organic chemical vapor deposition. The buffer was grown at 550 °C on a *c*-plane sapphire substrate. Trimethylgallium and ammonia were used as precursors. Cathodoluminescence (CL) and wavelength-dispersive x-ray spectroscopy (WDS) measurements were performed using an Oxford Instruments MonoCL2 scanning CL spectroscopy/imaging system and a Microspec WDS system both installed on a JEOL35C scanning electron microscope (SEM) equipped with a liquid-helium cold stage. The CL signal was dispersed by a 1200-lines/mm grating blazed at 500 nm and detected using a Hamamatsu R943-02 peltier cooled photomultiplier tube (PMT).

CL spectra, corrected for system response, obtained using a beam energy (E_b) of 15 keV and beam currents (I_b) of 0.5 nA at 300 K and 0.14 nA at 4 K are shown in Fig. 1. The room-temperature spectrum consists of a near-edge emission at 3.4 eV and the YL centered on 2.07 eV (FWHM=540 meV). The liquid-He spectrum consists of a donor-bound exciton (DX) emission⁸ at 3.46 eV (FWHM=20 meV) with a phonon replica at 3.39 eV, a donor-acceptor pair (DAP) with 2 LO phonon replicas⁸ at 3.25, 3.16, and 3.07 eV, respectively, the BL at ~2.8 eV and the YL at 2.24 eV (FWHM=450 meV), respectively. The features below 1.75 eV are second-order peaks. The DAP emission has been reported to be associated with O donors.⁷ The ripples visible in the BL and YL bands are due to the microcavity effect.⁹

Room-temperature CL kinetics profiles of the 3.4 eV, BL, and YL emissions are shown in Fig. 2(a). Liquid-He temperature (4 K) CL kinetics profiles of the DX, DAP, BL, and YL emissions are shown in Fig. 2(b). Each profile was obtained by blanking the electron beam, driving the sample to a previously unirradiated region and by recording the CL signal as a function of time as the sample was irradiated with a stationary electron beam ("spot mode"). The rate constants

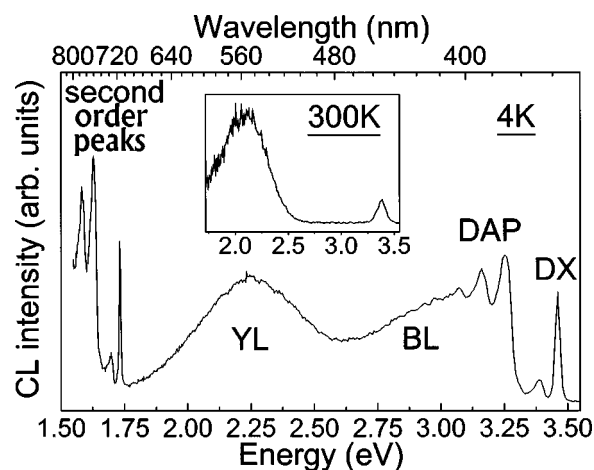


FIG. 1. CL spectra ($E_b = 15$ keV, corrected for system response) of autodoped GaN obtained at 4 K ($I_b = 0.14$ nA, band pass=1 nm) and 300 K (inset, $I_b = 0.5$ nA, band pass=2.5 nm). The high intensity of the second-order peaks is a system response correction artifact.

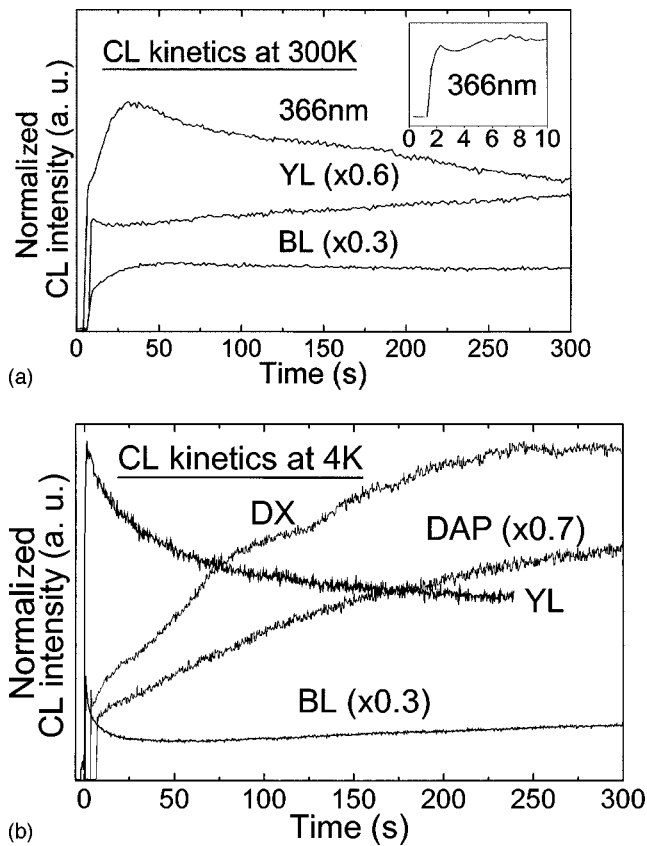


FIG. 2. CL kinetics ($E_b = 15$ keV) of (a) 3.4 eV, BL, and YL emissions at 300 K ($I_b = 3$ nA) and (b) DX, DAP, BL, and YL emissions at 4 K ($I_b = 6$ nA). The inset in (a) shows detail of the first 10 s of the 3.4 eV emission obtained using a lower electron dose ($I_b = 1.2$ nA).

of the kinetics curves increase with electron dose. The inset in Fig. 2(a) shows detail of the first 10 s of the kinetics of the 3.4 eV emission obtained using a lower electron dose. At 300 K, the profiles changed more rapidly than at 4 K due to a thermal contribution to the total energy of the sample. CL images obtained at 4 K using the DX, DAP, BL, and YL emissions after a 700 s spot-mode irradiation are shown in Fig. 3. The CL images (1024×800 pixels) were obtained using the minimum beam current (0.2 nA) and dwell time ($200 \mu\text{s}$ per pixel) to obtain a satisfactory S/N ratio while minimizing beam-induced effects during image acquisition. Noise in the kinetics profiles and asymmetries in the beam-induced features in the images are caused by a strong dependence of ion diffusion on the local charge trap density (impurity and defect concentration). The features discussed below represent typical, reproducible behavior.

Electron-beam irradiation of an uncoated semiconductor or insulator produces a positively charged region at the beam impact point due to a loss of charge through the emission of secondary electrons. The thin-positive region (of < 50 nm) is followed by a negative region produced by the electrons injected into the sample.¹⁰ The kinetics profiles in Fig. 2 are governed by (i) electron-beam-induced diffusion of species associated with the respective emissions and (ii) competitive recombination due to differences in recombination efficiencies between different luminescent centers.

We attribute the initial rapid, short-lived decrease of the

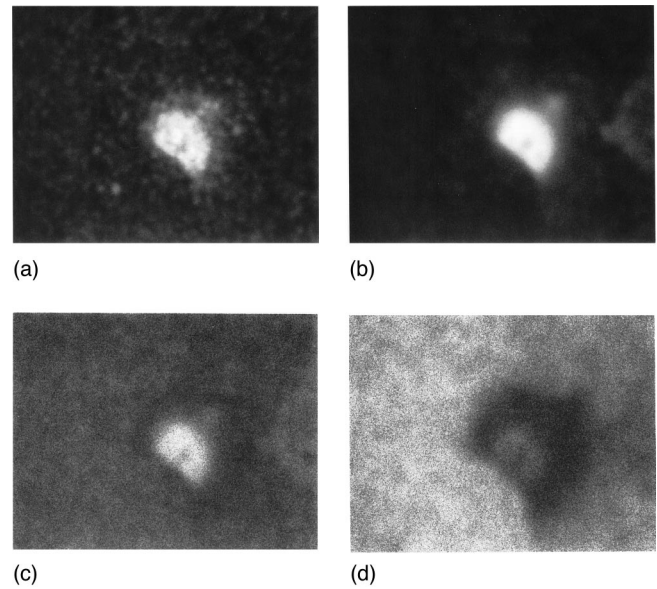


FIG. 3. CL images ($T = 4$ K, $E_b = 15$ keV, $I_b = 0.2$ nA, field of view = $42.5 \mu\text{m}$) of a region irradiated in spot mode ($I_b = 6$ nA) for 700 s acquired using (a) DX, (b) DAP, (c) BL, and (d) YL emissions.

3.4 eV [inset of Fig. 2(a)], DX [Fig. 2(b)] and YL [Fig. 2(a)] emission intensities to diffusion of H^+ from the positive, near-surface region into the negative region of the electron interaction volume. The H^+ ions are most likely to originate at hydrogenated gallium vacancies and at dangling bonds at the sample surface since interstitial hydrogen acts as an acceptor in n -type GaN and has a high-formation energy.¹¹ Consequently, dehydrogenation of V_{Ga} -related centers near the surface is followed by hydrogenation of V_{Ga} -related centers in the negative region of the interaction volume due to H^+ recapture at gallium vacancies. The YL intensity decreases because the majority of the detected YL signal is generated at a depth of approximately a quarter of the electron penetration range (~ 300 nm at 15 keV), where the primary electron-energy loss (and hence the electron-hole pair generation rate) maximizes.¹² The intensities of the 3.4 eV (at 300 K) and DX (at 4 K) emissions decrease because, unlike the YL, self-absorption in the sample causes the maximum of the detected 3.4 eV and DX generation profiles to shift from 300 to 80 nm below the surface,¹³ into the vicinity of the H-depleted near-surface region. CL generation directly in the H-depleted region is low due to nonradiative surface recombination. The initial decrease of the 3.4 eV and DX intensities reflects competitive recombination with YL centers, some of which are activated by H removal from gallium vacancies near the surface. The extent of the H^+ diffusion effect in spot-mode kinetics profiles was found to vary across the sample due to variations in H concentration as seen in the 3.4 eV curves in Fig. 2(a). The inhomogeneities in H concentration are probably caused by impurity congregation at extended defects and by deviations from thermodynamic equilibrium conditions during growth. The H diffusion effects in the kinetics profiles are short lived because, after the first few seconds of irradiation, O diffusion-related effects start to dominate the CL kinetics.

Diffusion of O_N^+ towards the negative region of the elec-

tron interaction volume causes an increase in (i) the 3.4 eV emission (over approximately the first 30 s at 300 K), (ii) the DX and DAP emissions (at 4 K) and (iii) the YL emission (at 300 K). The increase in the 3.4 eV and, to some extent, the DX emission corresponds to the removal of the $(V_{\text{Ga}}-\text{O}_\text{N})''$ complex contribution to YL in the vicinity of the positive near-surface region. The dissociation of $(V_{\text{Ga}}-\text{O}_\text{N})''$ complexes and consequent diffusion of $\text{O}_\text{N}^\bullet$ into the negative region of the interaction volume from the positive near-surface region and from outside the interaction volume leads to an increase in the concentration of $\text{O}_\text{N}^\bullet$ impurities in the region where most of the detected YL and DAP signals are generated. The surplus $\text{O}_\text{N}^\bullet$ impurities thus cause the YL (at 300 K), DAP (at 4 K), and to a lesser extent, the DX (at 4 K) intensities to increase. The contribution to the increase in DX intensity is low because of the nonlinear relationship between $\text{O}_\text{N}^\bullet$ concentration (~ 300 nm below the surface) and the measured increase in DX intensity, due to the exponential nature of self-absorption. At 4 K, the YL intensity decreases with irradiation time due to competitive recombination with the DAP and DX emissions and, to a lesser extent, due to the diffusion of H into the YL generation region. The DAP emission is not present at 300 K due to thermal ionization of $\text{O}_\text{N}^\bullet$.

The O-rich region in and around the negative region of the interaction volume is seen as the large bright feature in the CL images shown in Fig. 3. The region is larger than the diameter of the interaction volume [~ 2.6 μm at 15 keV (Ref. 13)]. Outside the interaction volume, $\text{O}_\text{N}^\bullet$ electromigration is assisted by breaking of O-related bonds by short wavelength GaN CL. The O-rich region is surrounded by an O-depleted region seen as a dark ring in the YL image, indicating where the O has diffused from. The absence of a dark ring in the DX image is caused by a contribution to the contrast by the recombination of free excitons since the free-exciton peak is too closed to the DX peak for it to be resolved in this experiment.⁸ The free-exciton signal maximizes in the O-depleted region due to minimization of competitive recombination with the O-related emissions. The absence of the dark ring in the DAP image can be explained by the acceptor distribution, assuming that the acceptor concentration is much lower than that of $\text{O}_\text{N}^\bullet$. This assumption is plausible in light of the low $\text{O}_\text{N}^\bullet$ and $(V_{\text{Ga}}-\text{O}_\text{N})''$ formation energies in *n*-type GaN.^{1,2} The DAP center concentration is hence governed by the concentration of the (negative) acceptors, which diffuse away from the negative region of the interaction volume. The acceptor involved in the DAP transition has been suggested to be C,⁷ consistent with first-principles calculations that show that the most energetically stable C state in *n*-type GaN is the $\text{C}_\text{N}^\bullet$ shallow acceptor.¹¹

The dark circle in the center of the bright oxygen halo seen in the CL images only appears after the 3.4 eV, DX, and DAP emissions stop increasing. We attribute it to accumulation of a C contamination layer and consequent CL absorption at the sample surface (around the beam impact point) and, to a lesser extent, to limited diffusion of negative ions (V_{Ga}'' and C_N') out of the interaction volume. The rates of increase of the YL (at 300 K) and DAP (at 4 K) kinetics profiles decay at lower rates due to the combined effects of (i) the ongoing increase in $\text{O}_\text{N}^\bullet$ concentration within the inter-

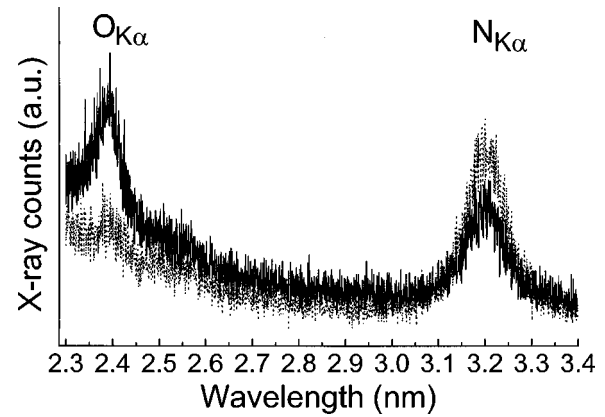


FIG. 4. Raw WDS spectra showing the $\text{O}_{K\alpha}$ and $\text{N}_{K\alpha}$ lines before (\cdots) and after (—) a 30 min spot mode irradiation ($E_b = 25$ keV, $I_b = 300$ nA).

action volume, (ii) the apparently low-diffusion rate of the anions and (iii) a decrease in CL absorption efficiency of C contamination (on the surface) with decreasing wavelength.

CL images acquired using the same beam parameters (as in Fig. 3) at room temperature using the 3.4 eV and YL emissions show similar contrast to the respective images obtained at 4 K. However, the extra thermal assistance available at 300 K manifests as an increase in the size of the regions affected by the diffusion processes. Also, at 300 K, the YL signal is much more intense in the O-rich region due to the reduced intensities of the (competitive) DX and DAP emissions.

The O diffusion model was verified by measuring the $\text{O}_{K\alpha}$ and $\text{Si}_{K\alpha}$ x-rays using WDS as a function of irradiation time. Si was not detected in the sample, satisfying the conditions necessary for high O content in *n*-type GaN.¹ In order to obtain a sufficiently strong $\text{O}_{K\alpha}$ signal, a beam energy of 25 keV and a beam current of 300 nA were used. Typical spectra showing the $\text{O}_{K\alpha}$ and $\text{N}_{K\alpha}$ lines acquired in spot mode before and after a 30 min irradiation are shown in Fig. 4. The intensity of the $\text{O}_{K\alpha}$ peak gradually increased and the $\text{N}_{K\alpha}$ decreased as a result of the irradiation. The $\text{N}_{K\alpha}$ decrease results from x-ray absorption by the C contamination layer induced by electron irradiation. The $\text{O}_{K\alpha}$ increase, caused by the diffusion of O into the interaction volume, is seen to dominate over $\text{O}_{K\alpha}$ absorption by the C contamination layer. Oxygen contamination, resulting from electron stimulated reactions involving residual gaseous O_2 within the SEM chamber, is unlikely as the chamber pressure is $< 10^{-6}$ Torr and the SEM is vented with dry N_2 . $\text{O}_{K\alpha}$ x rays generated in the substrate by Ga *L* lines are strongly absorbed by N in the GaN epilayer.

The increase in the BL kinetics profile at 300 K [Fig. 2(a)] appears to consist of a superposition of H- and O-related diffusion processes. We propose that the BL emission results from a transition from $\text{O}_\text{N}^\bullet$ to multiply hydrogenated V_{Ga}''' . The initial rapid increase in the first-few seconds is caused by hydrogenation of gallium vacancies in the negative region of the interaction volume. The slower increase over the first 50 s is due to the diffusion of $\text{O}_\text{N}^\bullet$ into the same region. After approximately 50 s, the rate of increase of H concentration in the negative region of the interaction volume becomes negligible and the BL intensity starts to gradually decrease due

to (i) competitive recombination at YL centers whose concentration continues to increase and (ii) preferential short wavelength CL absorption by the C contamination layer. The proposition of the dual roles of O_N^\bullet and V_{Ga}''' in BL and YL emissions is consistent with the contrast correlation in the BL and YL CL images at 4 K [Fig. 3]. BL images acquired at 300 K do not exhibit a dark ring in the O depleted region due to the reduction in the intensities of the DX and DAP emissions (relative to their intensities at 4 K) since the BL contrast is governed by the distribution of the less abundant (relative to O_N^\bullet) hydrogenated gallium vacancy acceptors. The rapid decrease in the BL kinetics profile at 4 K is caused by competitive recombination with the DX and DAP emissions.

In conclusion, the presented results illustrate electron-beam-induced charged impurity electromigration in wide band-gap semiconductors. Unlike narrow band-gap semicon-

ductors such as Si, GaAs, and Ge, impurity electromigration effects in wide band-gap materials can be significant and must be accounted for in interpretation of microanalysis data. The presented results illustrate the potential for controlled modification of charged impurity defect distributions in wide band-gap semiconductors by electron irradiation. Impurity diffusion studies can provide information regarding the roles of impurities in the optoelectronic properties of wide band-gap materials and devices. We employed time-resolved CL and WDS analysis of autodoped GaN to (i) directly confirm the roles of O_N^\bullet in bound exciton, donor-acceptor pair, and yellow emissions and (ii) illustrate the possible involvement of O_N^\bullet and hydrogenated gallium vacancies in the previously unexplained blue luminescence.

We gratefully acknowledge Dr. G. Li and Dr. J. Zou for providing the sample used in this study.

*On leave from Technical University of Berlin, Berlin, Germany.

†Corresponding author.

Electronic address: matthew.phillips@uts.edu.au

¹J. Neugebauer and C. G. Van de Walle, Appl. Phys. Lett. **69**, 503 (1996).

²T. Mattila and R. M. Nieminen, Phys. Rev. B **55**, 9571 (1996).

³W. Götz, N. M. Johnson, C. Chen, H. Liu, C. Kuo, and W. Imler, Appl. Phys. Lett. **68**, 3144 (1996).

⁴P. Perlin, T. Suski, H. Teisseyre, M. Leszczynski, I. Grzegory, J. Jun, S. Porowski, P. Boguslawski, J. Bernholc, J. C. Chervin, A. Polian, and T. D. Moustakas, Phys. Rev. Lett. **75**, 296 (1995).

⁵K. Saarinen, T. Laine, S. Kuisma, J. Nissila, P. Hautojarvi, L. Dobrzynski, J. M. Baranowski, K. Pakula, R. Stepniewski, M. Wojdak, A. Wyszomolek, T. Suski, M. Leszczynski, I. Grzegory,

and S. Porowski, Phys. Rev. Lett. **79**, 3030 (1997).

⁶C. G. Van de Walle, Phys. Rev. B **56**, 10 020 (1997).

⁷M. Leroux, B. Beaumont, N. Grandjean, P. Lorenzini, S. Haffouz, P. Vennegues, J. Massies, and P. Gibart, Mater. Sci. Eng., B **50**, 97 (1997).

⁸J. W. Orton and C. T. Foxon, Rep. Prog. Phys. **61**, 1 (1998).

⁹A. Billeb, W. Grieshaber, D. Stocker, E. F. Shubert, and R. F. Karlicek Jr., Appl. Phys. Lett. **70**, 2790 (1997).

¹⁰J. Cazaux, J. Appl. Phys. **59**, 1418 (1986).

¹¹J. Neugebauer and C. G. Van de Walle, Phys. Rev. Lett. **75**, 4452 (1995).

¹²M. Toth and M. R. Phillips, Scanning **20**, 425 (1998).

¹³K. Fleischer, M. Toth, M. R. Phillips, J. Zou, G. Li, and S. J. Chua, Appl. Phys. Lett. (to be published).